Proceedings of the 9th U.S. National and 10th Canadian Conference on Earthquake Engineering
Compte Rendu de la 9ième Conférence Nationale Américaine et
10ième Conférence Canadienne de Génie Parasismique
July 25-29, 2010, Toronto, Ontario, Canada • Paper No 1252

REPAIR COST ANALYSIS OF MULTISTORY BUILDINGS WITH PRECAST CONCRETE CLADDING

J. Hunt[1] and B. Stojadinovic[2]

ABSTRACT

Recent probabilistic evaluations have shown that the repair costs for typical multistory buildings after minor and moderate earthquakes are heavily influenced by the amount of non-structural damage. However, most of the efforts in non-linear dynamic modeling focus on representing the behavior of structural elements and do not include the effects of non-structural elements. An important non-structural element is the exterior cladding system. In this paper, the analytical model of a typical cladding design is created, and the damage states of the cladding components are identified from experimental data and analytical models. The damage state models translate the engineering demand parameters of the cladding system to probabilities of exceeding a certain damage state. The majority of damage to cladding occurs in the caulking between panels, the window system components, and the connections between the cladding panels and the structure. The damage models show that the cladding system can become significantly damaged even in a low-level earthquake. These data, along with repair quantities and unit repair costs, are used to calculate the distribution of the total post-earthquake repair costs of the cladding system following the PEER PBEE methodology.

Introduction

The design of cladding systems and their connections are typically an afterthought in structural engineering, as this task is usually handed off to the cladding sub-contractor. Furthermore, structural engineers usually assume that the cladding system does not participate in the lateral resisting system of the building during seismic events. However, analytical and experimental studies have shown that exterior precast cladding panels do interact with the supporting structural framing, causing unexpected failure modes to both the cladding system and the structural frame (Wolz et al., 1992; Henry and Roll, 1986; Goodno et al., 1983; Hunt and Stojadinovic, 2008). The connections between the cladding panels and the structural frame largely determine the amount of damage that the cladding system sustains in an earthquake. For example, engineers typically use flexible connections (long threaded rods) or connections with

---
[1]Graduate Student, Dept. of Civil and Environmental Engineering, University of California-Berkeley, Berkeley, CA
[2]Professor, Dept. of Civil and Environmental Engineering, University of California-Berkeley, Berkeley, CA

built-in tolerances (slotted bolted connections) to isolate the cladding system from the frame. However, these connections often do not behave as intended, and damage to the cladding system happens at far lower seismic hazard levels than expected.

A detailed analytical model of a typical cladding system was created to calculate its seismic response and to provide a basis to determine expected damage states and repair costs. The PEER performance-based earthquake engineering (PBEE) methodology (Mackie et al., 2007; Moehle et al., 2005) was used to structure the repair cost calculation. In the following sections, the damage states are described as observed from experimental data and analytical modeling.

Description of Cladding System

The nine-story Los Angeles SAC building was selected as the study building. The structure has nine stories above ground and is five bays wide in each direction. The cladding system consists of spandrel panels at each floor level and column cover panels that span between floors. A three-dimensional view of the building is shown on the left side of Fig. 1, and a typical elevation of the cladding system is shown on the right side of Fig. 1.
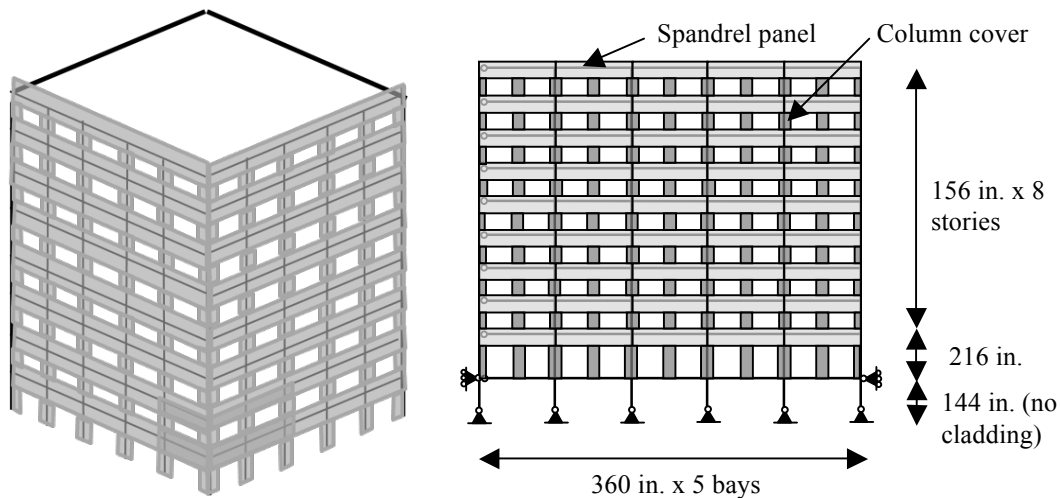
Figure 1. Isometric view (left) and elevation (right) of 9-story SAC building (1 in. = 25.4 mm)

A detailed elevation of the cladding system is shown in Fig. 2. The spandrel panels, made of normal-weight concrete, are each 360 wide by 78 inches high by 5 inches thick. They are connected to the exterior columns with push-pull threaded connections (four per panel), shown as black circles in Fig. 2. The threaded rods are embedded in the spandrel panels and then connected to the columns with hollow tube sections. The spandrel panels are connected to the beam/slab with rigid lateral connections (one per panel), shown as black squares. The rigid connection consists of a plate embedded in the spandrel panel and welded to a plate embedded in the deck. The self-weight of the spandrel panel is supported by vertical bearing connections (two per panel), shown as black triangles. The vertical bearing connection consists of a leveling bolt between the panel and the deck.
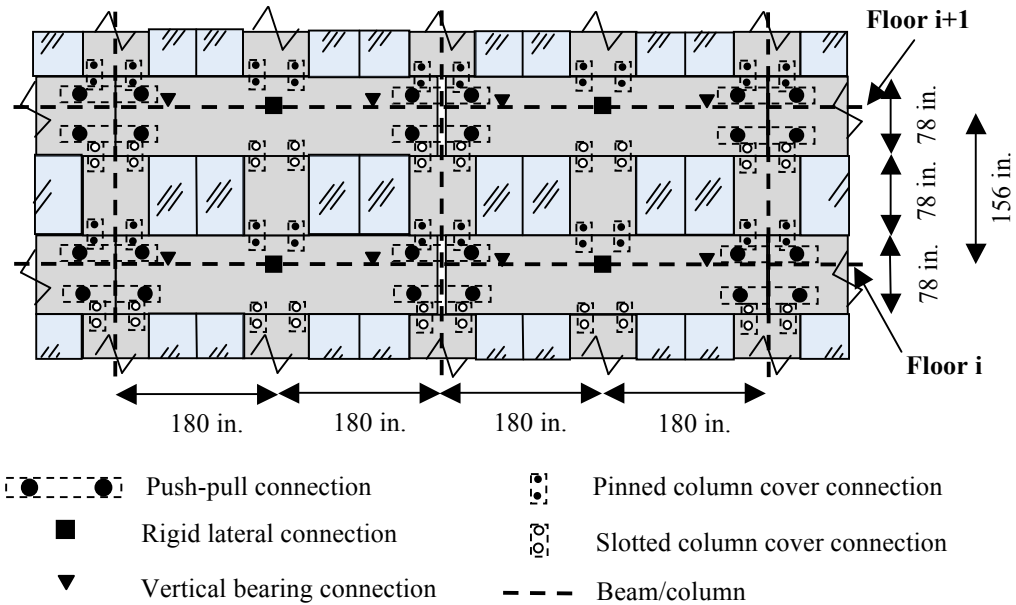
Figure 2. Elevation of the cladding system and connection types (1 in. = 25.4 mm)

The column cover panels, made of normal-weight concrete, are each 54 inches wide by 78 inches high by 5 inches thick. They are connected to the spandrel panels and not to the structural framing. The bottom connections are made of two pin-bolted connections, and the top connections consist of horizontally slotted bolted connections.

The window system is a dry-glazed, narrow mullion design with two window panes per opening, as shown in Fig. 2. Aluminum window framing is secured to the cladding panels, and the window panes are secured to the frame with rubber gaskets.

The mass of the cladding system (including the panels, connectors, and window system) accounts for approximately 14% of the total seismic mass of the building.

Engineering Demand Parameters

A nonlinear analytical model of the study building and cladding was created in OpenSees (Hunt and Stojadinovic, 2008), and time-history analyses were run to determine the response of the building and cladding system to earthquake ground motions. Rayleigh damping of 3% was enforced at the first mode period and a period of 0.2 sec. The fundamental period of the building was found to be 2.13 sec. A suite of 120 motions of varying magnitudes and distances were selected and uniformly scaled by a factor of 2.0. The selected earthquakes had magnitudes ranging from 5.5 to 7.5 Mw and closest distances to fault rupture from 0-65 km. Response quantities such as interstory drift, residual drift, and cladding connector deformations were recorded. For example, in Fig. 3, the maximum interstory drift in story 5 and the maximum push-pull connector deformation in story 5 are plotted against the spectral acceleration at the first mode vibration period of the bare frame model. A clear linear trend is observed when the quantities are plotted in log-log space.
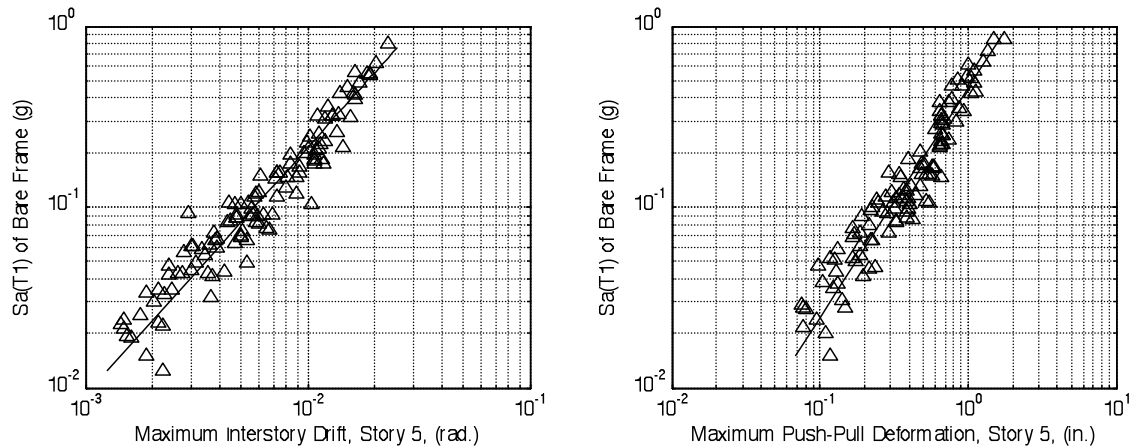
Figure 3. Maximum interstory drift (left) and push-pull deformation (right) at story 5 plotted against spectral acceleration (1 in. = 25.4 mm)

Cladding Damage States

There are several types of damage associated with cladding failure, including those related to the caulking between the cladding panels, the components of the window glazing, and the connections between the cladding panels and the structural frame. Little to no damage is expected in the precast panels themselves due to their thickness and rigidity. As such, the panels are modeled to behave as rigid blocks, and the damage to the cladding system is concentrated in the connectors and window glazing.

Caulking

Silicone caulking is used to seal the joints between the panels and provide a watertight and airtight cladding system. The caulking must accommodate the interstory drift between adjacent spandrel panels and column covers. According to Mark Hildebrand at Willis Construction, a local precast cladding fabricator, most types of caulking used in cladding show hairline cracking at 0.75 inches of shear displacement (0.005 rad. interstory drift ratio assuming a story height of 13 ft.) and become debonded after 1.5 inches of shear displacement (0.01 rad. interstory drift ratio). Since the building's joints are re-caulked approximately every 10-20 years due to deterioration and fading, all caulking is expected to be replaced if approximately 50% or more of the caulking is damaged.

Window Glazing System

The main components of interest in the window system are the glass panels, rubber gaskets, and the aluminum window framing. The details in Fig. 4 show the horizontal sill jamb, the vertical mullion, and the horizontal head jamb. Several dynamic racking tests of this design were performed by Behr et al. (1995) and Behr and Worrell (1998), and the results are used to identify the damage states of the window system.
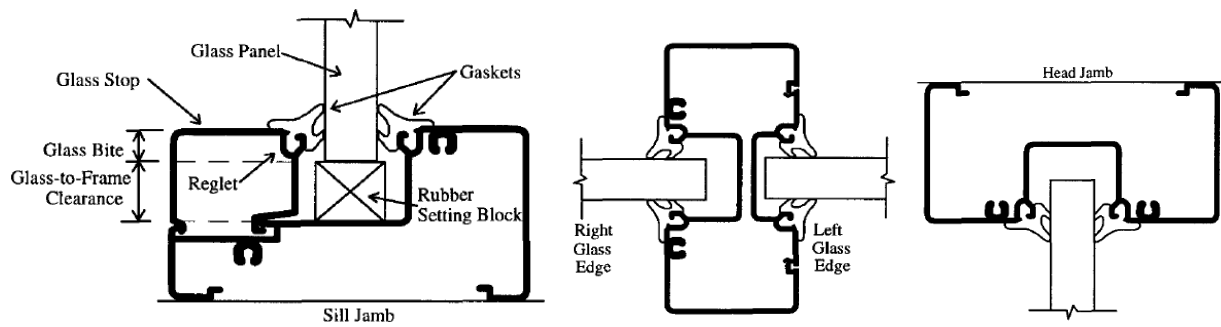
Figure 4. Cross-sections of window system: horizontal/sill (left), mullion (middle), and horizontal/head (right)

Glass Panels

The glass panels, each 5 feet wide and 6 feet high, are 1-inch annealed insulating glass units and 1-inch heat-strengthened insulating glass units, depending on the location in the building. During dynamic racking, glass panels may come into contact with the window framing, causing damage to the corners of the glass in the form of glass fragmentation and perimeter cracking. For the relevant glass types, Behr et al. (1995) report an average length of 1.6 inches of edge damage occurring at drifts at or below 0.94 inches (0.006 rad. interstory drift ratio). The edge damage was not sufficient enough to warrant immediate glass replacement; however, the damage may cause long-term serviceability problems, such crack propagation due to thermal and wind stresses.

The second type of damage that may occur to the glass panel is translation and rotation of the panel within the window framing. At 1.7 inches drift (0.011 rad. interstory drift ratio), Behr et al. (1995) report an average horizontal translation at the center of the glass panel of 0.21 inches and an average rotation at the center of the glass panel of 0.22 degrees. These movements result in 0.33 inches of total horizontal movement at one of the corners, which is very close to the initial glass bite (portion of the glass that extends into the glazing pocket) of 3/8 inch on all sides. Thus, the glass is very close to being completely pulled out of the glazing pocket, posing a risk to air and water infiltration. The glass panels may have to be deglazed, repositioned, and reglazed to restore sufficient glass bite.

The third and fourth types of damage are major crack formation and glass fallout. For 1-inch annealed insulating glass units, Behr and Worrell (1998) report that observable cracking occurred at an average drift of 2.5 inches (0.016 rad. interstory drift ratio), and glass fallout occurred at a drift of 3.1 inches (0.02 rad. interstory drift ratio).

The allowable drift for window glazing determined from design codes is based on the glass pane dimensions and clearances between the glass pane and framing. Using Equation 6.3-2 in FEMA 450, the allowable drift limit (in the design level earthquake) of 5 ft. wide by 6 ft. tall window panes with 1/2-in. of clearance around the perimeter is 2.2 in. From the time-history analyses (Fig. 3), the mean value of the maximum drift for the design level earthquake ($Sa(T_1)$ = 0.34g) is approximately 2.3 in. (0.015 rad.). Thus, the interstory drifts expected in the design level earthquake slightly exceed the allowable drift limit imposed by FEMA 450. Based on the data from the experimental tests, the glass panes are expected to show perimeter cracking and

some glass panes are expected to translate and rotate within the framing in the design level earthquake. However, no major glass fallout is expected since the fallout capacity of the glass exceeds the expected interstory drifts from the time-history analyses.

Gaskets

The glass panes are dry-glazed to the window framing pocket using interior and exterior rubber Santoprene gaskets. The gaskets create a tight seal to ensure water and air tightness of the glazing system. However, during dynamic racking, the seals may become dislodged from their seat or pushed into the glazing pocket from the moving glass. At 1.7 inches drift (0.011 rad. interstory drift ratio), the average lengths of distorted, pulled-out, pushed-in, or shifted gaskets around the perimeter of the glazing varied between 23 and 34 inches.

Framing and Mullions

The aluminum framing and mullions are expected to sustain little damage during dynamics racking. Behr et al. (1995) commented that the little damage that occurred was limited to gouging of the aluminum glazing pocket from the corners of the glass panels.

Cladding Connectors

As discussed previously, the cladding connectors of focus are the threaded rods (push-pull connections) that attach the spandrel panels to the columns and the column cover connectors that bolt the column cover panels to the spandrel panels. These two types of connections are expected to sustain most of the damage.

Push-pull connectors

Static tests of threaded rods were conducted by McMullin et al. (2004). The threaded rods are embedded in the spandrel panel and are bolted through the hollow tube section attached to the column; therefore, the end conditions are assumed to be fixed. The rods were subjected to in-plane shear deformation between the spandrel panel and columns. The effective rod length is assumed to be 8 inches, and the diameter is 1.0 inch. The maximum force before fracture was approximately 6.0 kips (26.7 kN) at a deformation of 2.2 inches.
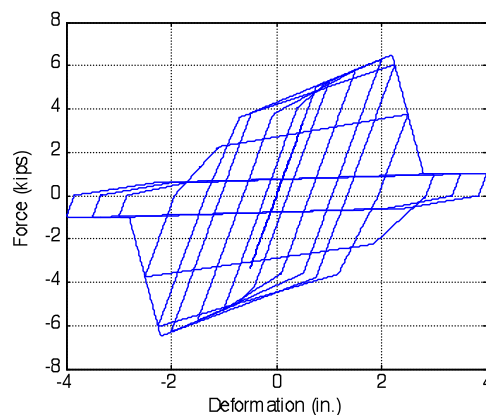
Figure 5. Force-deformation curve of push-pull connector (1 in. = 25.4 mm.; 1 kip = 4.45 kN)

The cyclic force-deformation relationship, shown in Fig. 5, was created using the results of the static tests. Yielding of the rod occurs due to double curvature bending at 0.75 inches deformation and 4.0 kips (17.8 kN). Significant yielding develops at 1.25 inches, and failure occurs at approximately 2.2 inches.

Column Cover connectors

The column cover panels are connected to the spandrel panels at adjacent floor levels with pin-bolted connections at the bottom and slotted connections at the top. The force deformation relationships for these single-bolted connections, shown in Fig. 6, are derived from test data by Crawford and Kulak (1968). The top connector consists of a one-inch bolt in a 4.0 inch slotted hole, resulting in 1.5 inches of gap on either side of the bolt. Thus, the force-deformation relationship is offset from the origin by 1.5 inches.
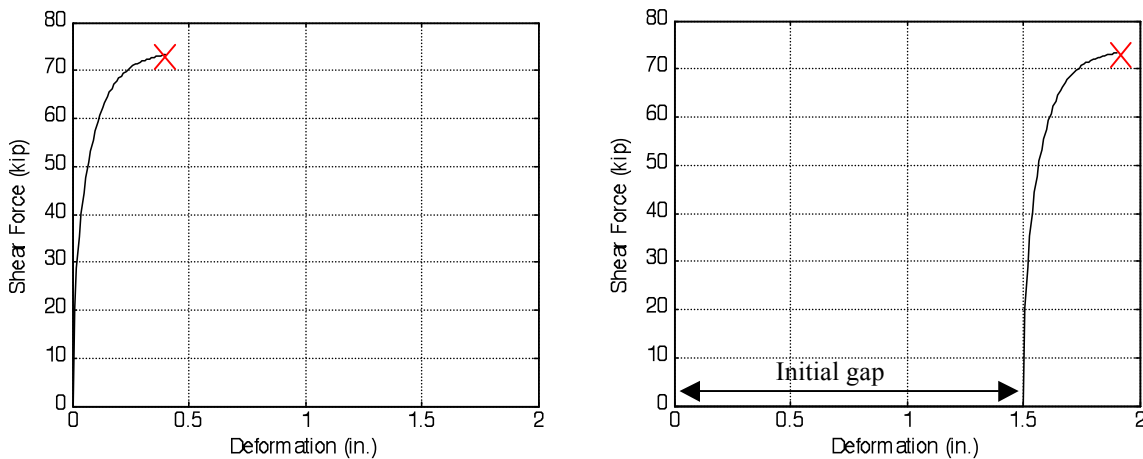
Figure 6. Force-deformation relationship of bottom (left) and top (right) column cover connectors (1 in. = 25.4 mm.; 1 kip = 4.45 kN)

The initial yield point occurs at 0.068 inches of deformation, with significant yielding occurring at 0.22 inches. The overall behavior is fairly brittle, with fracture occurring at a connector deformation of 0.33 inches.

Summary of Damage States

The damage state thresholds of the cladding are summarized in Table 1 below. A lognormal distribution is used to describe the cumulative probability of exceeding each damage state. In Table 1, the median values λ of the engineering demand parameter (EDP) are given for each damage state along with a shape parameter β for the lognormal distribution (a larger β represents more uncertainty). The values of β were based on engineering judgment and limited statistical information from the experimental tests. The parameters in Table 1 are used to define the damage state fragility curves for each component, shown in Figs. 7 and 8.

The values given in Table 1 correspond to the thresholds between different damage state

regions. For a given cladding component, the DS0 region represents damage that typically requires no repair, and the DS∞ region represents damage beyond the last failure mode, for which no incremental costs are accrued since the item is already damaged to beyond the point of complete replacement. The addition of these two boundary damage states help to completely define the failure modes and aid in the repair cost calculations.

Table 1. Summary of damage states to cladding system (1 in. = 25.4 mm.)

Component	Engineering Demand Parameter (EDP)	Damage State (DS) and corresponding EDP values of median (λ) and shape parameter (β)			
		DS 0	DS 1	DS 2	DS 3
Caulking between column cover and spandrel panels at story i	Interstory drift ratio at story i	Initial cracks $\lambda = 0.005$ rad., $\beta = 0.15$	Debonding failure $\lambda = 0.01$ rad., $\beta = 0.25$	-	-
Window system at story i	Interstory drift ratio at story i	Edge cracking at glass perimeter $\lambda = 0.006$ rad., $\beta = 0.12$	Glass translation and gasket pullout $\lambda = 0.011$ rad., $\beta = 0.20$	Major glass cracking $\lambda = 0.016$ rad., $\beta = 0.19$	Glass panel fallout $\lambda = 0.02$ rad., $\beta = 0.16$
Push-pull connectors	Connector shear deformation	Initial yielding $\lambda = 0.75$ in., $\beta = 0.25$	Significant yielding $\lambda = 1.25$ in., $\beta = 0.25$	Fracture $\lambda = 2.2$ in., $\beta = 0.25$	-
Column-cover connectors	Connector shear deformation	Initial yielding $\lambda = 0.068$ in., $\beta = 0.19$	Significant yielding $\lambda = 0.22$ in., $\beta = 0.11$	Fracture $\lambda = 0.33$ in., $\beta = 0.10$	-
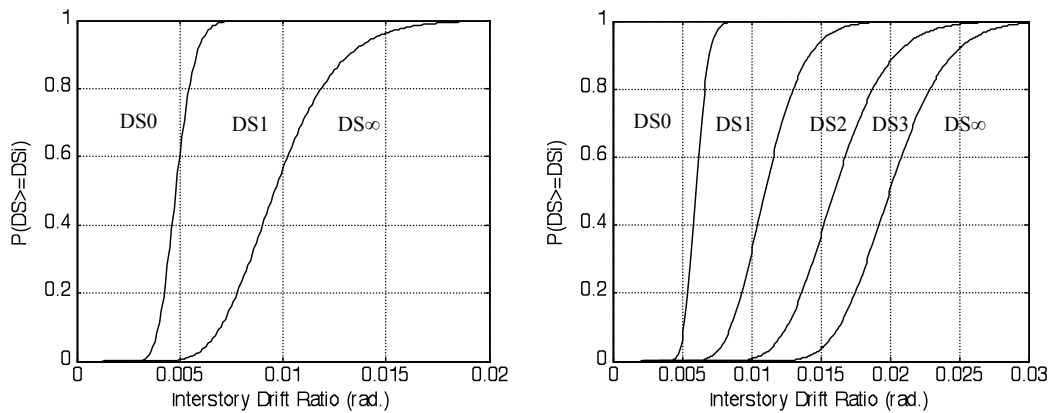
Figure 7. Damage state fragility curves: (left) panel joint caulking and (right) window system components (1 in. = 25.4 mm.)
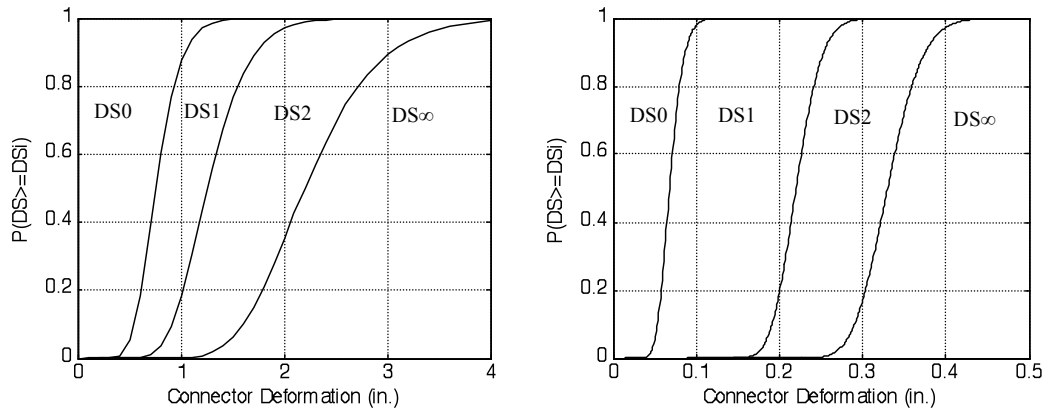
Figure 8. Damage state fragility curves: (left) push-pull connectors and (right) column cover
connectors (1 in. = 25.4 mm.)

Conclusions

The behavior of the cladding system has significant implications on the post-earthquake repair costs of multistory buildings. Since up to 80% of the initial cost of a typical multistory office building is comprised of nonstructural components, damage to the cladding system can generate large economic losses for the building owner. In this paper, a detailed analytical model of a nine-story building was presented. The response of the cladding system was recorded for a suite of 120 ground motions covering a range of seismic intensities. A damage analysis of the cladding system was performed by considering experimental data and analytical modeling of the cladding components. With these data, the distribution parameters were determined for the damage state fragility curves. Repair quantities can be estimated from the experimental tests, and the unit repair costs will be determined from local cladding fabricators. The PEER PBEE method will be used to calculate the distribution of the total repair cost for different levels of seismic intensities. Preliminary analyses using the damage data in this paper have shown that the total repair cost of the cladding system for the design level earthquake (10% probability of exceedance in 50 years) is about $2 million, representing approximately 40% of the replacement cost of the cladding. Furthermore, the repair cost of the cladding system at the design level earthquake represents approximately 30% of the total repair cost of the complete building. The overall aim of this research is to bring the earthquake engineering community one step closer to understanding how the building envelope behaves in an earthquake and to push for more resilient and cost-effective cladding designs.

Acknowledgments

References

Behr, R. A., Belarbi, A., and Brown, A. T., 1995. Seismic Performance of Architectural Glass in a Storefront Wall System, *Earthquake Spectra* 11(3), 367-391.

Behr, R. A and Worrell, C. L., 1998. Limit States for Architectural Glass Under Simulated Seismic Loadings, in *Proc. of Seminar on Seismic Design, Retrofit, and Performance of Nonstructural Components, ATC-29-1 January 22-23, 1998*, San Francisco, CA, pp. 229-240.

Goodno, B.J., Craig, J.I., and Meyyappa, M., 1983. Cladding-Structure Interaction in High-Rise Buildings. *Report No. CEE-7704269*, Georgia Institute of Technology, Atlanta, GA, January.

Henry, R. M. and Roll, F., 1986. Cladding-Frame Interaction, *Journal of Structural Engineering* 112(4), 815-834.

Hunt, J., and Stojadinovic, B., 2008. Nonlinear Dynamic Model for Seismic Analysis of Non-structural Cladding, In *Proceedings of the Fourteenth World Conference on Earthquake Engineering*, Beijing, China, October 12-17.

Mackie, K.R., Wong, J.M., and Stojadinovic, B., 2007. Integrated Probabilistic Performance-Based Evaluation of Benchmark Reinforced Concrete Bridges, *Technical Report PEER 2007/09*, Pacific Earthquake Engineering Research Center, University of California, Berkeley, California.

McMullin, K., Wong, Y., Choi, C., Chan, K., 2004. Seismic Performance States of Precast Concrete Cladding Connections, *Proceedings of 13th World Conference on Earthquake Engineering*, Vancouver, B.C., Canada, August 1-6, Paper No. 3379.

Moehle, J., Stojadinovic, B., Der Kiureghian, A., Yang, T. Y., 2005. An Application of the PEER Performance-Based Earthquake Engineering Methodology, *PEER Research Digest 2005-1*, August.

Wolz, M., Hsu, C. C., and Goodno, B. J., 1992. Nonlinear Interaction between Building Structural Systems and Nonstructural Cladding Components, *Proceedings of ATC-29 Seminar and Workshop on Seismic Design and Performance of Equipment and Nonstructural Elements in Buildings and Industrial Structures*, 329-340.